Applied Catalysis B: Environmental 342 (2024) 123431

Contents lists available at ScienceDirect

Applied Catalysis B: Environmental

journal homepage: www.elsevier.com/locate/apcatb

Photobiocatalytic conversion of solar energy to NH_3 from N_2 and H_2O under ambient condition

Nuttavut Kosem [a,*], Xiao-feng Shen [b], Yutaka Ohsaki [c], Motonori Watanabe [b,c], Jun Tae Song [c], Tatsumi Ishihara [a,b,c]

[a] Department of Applied Chemistry, Faculty of Engineering, Kyushu University, 744 Motooka, Nishi-ku, Fukuoka 819-0395, Japan
[b] Department of Automotive Science, Graduate School of Integrated Frontier Sciences, Kyushu University, 744 Motooka, Nishi-ku, Fukuoka 819-0395, Japan
[c] Mitsui Chemicals, Inc. Carbon Neutral Research Center (MCI-CNRC), International Institute for Carbon-Neutral Energy Research (I2CNER), Kyushu University, 744 Motooka, Nishi-ku, Fukuoka 819-0395, Japan

ARTICLE INFO

Keywords:
Cyanobacteria
Anabaena variabilis
Photobiocatalysis
Nitrogenase
Ammonia

ABSTRACT

NH_3 is an important chemical fertilizer and expecting as H_2 carrier. Several methods have been investigated for eco-friendly NH_3 production under mild conditions instead of Haber-Bosch process using 400 °C, 20 MPa. Here, cyanobacterial Anabaena variabilis was utilized as a nitrogenase-producing biocatalyst that converts N_2/H_2O to NH_3 under ambient conditions. Biocatalytic reactions revealed that $MV^{\bullet+}$ can penetrate cell membrane and transfer electrons generated in inorganic photocatalyst. We first reported photobiocatalytic NH_3 production of cyanobacteria and TiO_2. Comparing with natural system, NH_3 formation rate of the hybrid system increased 81.3 times with an initial rate of 2031.7 $nmol{\cdot}h^{-1}$ and turnover number of 216.8.

1. Introduction

Currently, most NH_3 is produced by the Haber-Bosch process, in which hydrogen (H_2) and nitrogen (N_2) gases are converted into NH_3 under severe condition, high temperatures and pressure (typically 350–550 °C and 150–300 atm) [1,2]. NH_3 is an important chemical fertilizer and chemical intermediate for industrial production. However, the process consumes around 2 % of global energy annually and is responsible for roughly 3 % of all anthropogenic greenhouse gas (GHG) emissions [3]. Due to growing concern and awareness about global warming, new environmental-friendly process under more mild conditions is strongly required. However, many alternative technologies are still low efficiency, cost, and poor selectivity [4,5]. Finding sustainable and highly efficient processes including efficient catalysts is still a challenging issue.

In contrast, the ability to synthesize NH_3 is found in various species in nature, especially some prokaryotes and cyanobacteria under ambient conditions. Nitrogenase is the only biocatalytic enzyme to fix and break the strong N≡N triple bond of N_2 to NH_3 as follows [6]:

$$N_2 + 16MgATP + 8H^+ + 8H^- \xrightarrow{[MoFe]-Nitrogenase} 2NH_3 + H_2 + 16MgADP + 16Pi$$

Although N_2-fixing microorganisms can liberate extracellular NH_3 without GHG formation and high energy requirement, nitrogen metabolisms are tightly controlled to maintain the intracellular C-N equilibrium and amino acid pools homeostasis [7]. Due to low productivity of natural NH_3 synthesis via the activities of nitrogenase and ATP-dependent photosystem I, the replacement by inorganic photosystem is thus the objective of this study.

In nature, N_2 is reduced by nitrogenase in heterocyst of filamentous cyanobacteria activated by ATP which is synthesized from photosystem I (PSI) and sucrose obtained from Calvin cycle in vegetative cells. So, in natural photosynthesis, Calvin cycle in vegetative cells is important to generate energy and protein of cyanobacteria. The number of heterocyst cells is limited and the activation of N_2 to NH_3 occurs after light reaction in vegetative cell [8–11]. In this study, N_2 activation on hydrogenase is investigated by direct injection of redox mediator of MV^{2+} into heterocyst cells which is charge transfer of photoexcited electron in TiO_2 for achieving the high NH_3 formation rate.

The purification processes of oxygen-labile nitrogenase are complicated, costly, and time-consuming. Application of whole-cell system is a more convenient option and effective to use oxygen-sensitive enzymes under more stable conditions. In addition, self-recovery of biocatalyst is also possible after reaction. Among various species, photoautotrophic

* Corresponding author.
E-mail address: kosem_k@i2cner.kyushu-u.ac.jp (N. Kosem).

https://doi.org/10.1016/j.apcatb.2023.123431
Received 20 August 2023; Received in revised form 12 October 2023; Accepted 21 October 2023
Available online 24 October 2023
0926-3373/© 2023 Elsevier B.V. All rights reserved.

cyanobacteria with the *nif* gene clusters of nitrogenase expression show the potential for use as whole-cell biocatalysts [12–14]. Unlike free nitrogenase, oxygen-impermeable heterocyst differentiated in nitrogen-deficient medium protects intracellular nitrogenase from aerobic environment [15,16].

According to the biological properties of cyanobacteria, this study aims to establish the photobiocatalytic system for NH_3 production using light energy. TiO_2 is served as a light-absorbed photocatalyst, while an N_2-fixing cyanobacterium Anabaena variabilis acts as a whole-cell biocatalyst. The development of TiO_2:cyanobacteria hybrid systems operating under ambient conditions is a promising strategy for sustainable NH_3 production from N_2 to H_2O.

2. Materials and methods

2.1. Chemicals

Glycerol (Chameleon Reagent), methyl viologen dichloride (1,1′-dimethyl-4,4′-bipyridinium dichloride, Tokyo Chemical Industry Co., Ltd), benzyl viologen dichloride (1,1′-dibenzyl-4,4′-bipyridinium dichloride, Sigma-Aldrich), P-25 TiO_2 (Nippon Aerosil Co., Ltd), sodium dithionite (Sigma-Aldrich), L-methionine sulfoximine (MSX, Sigma-Aldrich) and ammonium chloride (nacalai tesque) were purchased from commercial manufacturers. Iron, nickel and molybdenum standards were obtained from Merck. All chemical reagents were utilized without further purification. To cultivate cyanobacteria, BG11 broth and Trace Metal Mix A5 with Co were purchased from Sigma-Aldrich. Allen & Arnon medium was prepared by adding disodium molybdate (VI) dihydrate (Na_2MoO_4, nacalai tesque). High-purity water (<0.055 μS/cm) was supplied by an ultrapure water system (RFU424TA, Advantec) for all chemical preparations.

2.2. Photocatalytic reduction of viologens by TiO_2

The reaction mixture included 100 mM glycerol at pH 7, 2.5 mg/mL TiO_2 and 10 mM viologen (V^{2+}). The reaction was conducted in a 10 mm × 10 mm quartz cuvette with a screw cap with a polytetrafluoroethylene/silicone septum. O_2 was displaced by bubbling N_2 gas through the solution for 2 min. The reaction was initiated by light irradiation under a 300-W xenon lamp (CX-04E with an R300-3J lamp housing, INOTEX Co., Ltd., Japan). The cuvette was then centrifuged at 1,000g for 1 min to avoid the diffusion of TiO_2 powder. The absorption spectra were monitored using a UV-Vis spectrophotometer (SH-1000Lab, Corona Electric Co., Ltd., Japan). The amount of reduced $MV^{\bullet+}$ formed was calculated from the absorbance at 605 nm using a molar conversion coefficient, ε, of 1.3×10^4 $M^{-1}cm^{-1}$ [17,18], while the amount of reduced $BV^{\bullet+}$ was estimated using a molar conversion coefficient, ε, of 0.74×10^4 $M^{-1}cm^{-1}$ from the absorbance at 550 nm [19].

2.3. Cultivation of cyanobacteria

A. variabilis ATCC 29413 was obtained from American Type Culture Collection. Cyanobacterial cells were aerobically cultivated in either BG11 medium supplemented with Trace Metal Mix A5 with Co or Allen & Arnon (AA) medium supplemented with 20 μM Na_2MoO_4 under the light intensity of 5000 Lux (68 μmol/m^2/s) at 26 °C and 140 rpm shaking incubator. At a cell density of 1.0 at A_{683} and chlorophyll a (Chl a) content of ~12 μg/mL, cyanobacterial cells were harvested by centrifugation at 10,000*g* for 5 min for experiments.

2.4. Heterocyst differentiation

Different culture systems can affect the differentiation of heterocysts. Filamentous cyanobacteria were stained with 0.5 % Alcian blue, which binds specifically to the polysaccharide layer of heterocyst envelopes [20]. Heterocyst frequency was counted directly using a microscope and averaged as a percentage of every 100 cell counts. Cyanobacterial morphology was captured and counted with a laser microscope (Keyence, Tokyo, Japan).

2.5. Determination on metal ion contents

To estimate the presence of intracellular [MoFe]-nitrogenase, iron (Fe), nickel (Ni) and molybdenum (Mo) contents were measured by an inductively coupled plasma-atomic emission spectroscopy (ICP-AES) [21]. After cultivation, cell pellets were collected by centrifugation at 10,000g for 5 min and washed twice with deionized distilled water to remove extracellular metal contents. The pellets were mechanically digested by the sonication methods and freeze-thaw for 5 cycles in liquid N_2 for 1 min and a 37 °C-water bath for 5 min. The concentrations of metal ion contents in the crude cell extracts were quantified based on the calibration curves of standard elements of Fe, Ni and Mo.

2.6. Acetylene reduction assay

Acetylene reduction test has been widely used to determine both in vivo and in vitro nitrogenase activity [22]. In a 10-mL glass vial sealed with rubber stopper and aluminium cap, a 100 mg cell mass of cyanobacteria was resuspended in either 5 mL of culture medium or 50 mM Tris-HCl pH 7 and incubated under 5 % acetylene in 95 % N_2 atmosphere. After incubating under the light intensity of 5000 Lux (68 μmol/m^2/s), 26 °C and 140 rpm shaking incubator, a 500 μL of gas sample was collected from a headspace of the reaction vial by a gas-tight syringe and injected into a gas chromatography (GC-8APF, Shimadzu Corp., Japan). Acetylene reduction and ethylene production were detected by GC equipped with a hydrogen flame ionization detector and a 3.2 mm, 2-m long column containing 80–100 mesh Pora-pak U (Chrompak). The injector/detector and oven temperature was 180 °C and 110 °C, respectively. Argon was used as a carrier gas. Triplicate samples were determined from each condition for average data.

2.7. Biocatalytic reaction of cyanobacteria

After cultivation, cyanobacterial cells were freshly harvested and washed by 50 mM Tris-HCl at pH 7. Viologen-dependent biocatalytic activity was initiated by adding 10 mM reduced $V^{\bullet+}$ (V^{2+} dissolved in $Na_2S_2O_4$ solution) into the 100-mL reactor containing a 5-g cell mass of cyanobacteria suspended in 50 mM Tris-HCl pH 7 under N_2 atmosphere. During the experiments, H_2 / N_2 in a gas phase and NH_3 in a liquid phase were simultaneously measured at each time point.

2.7.1. H_2 and N_2 determinations by gas chromatography

In time-course sampling, H_2 production and N_2 consumption were monitored by a gas chromatograph (GC-8A, Shimadzu Corp., Japan) equipped with a thermal conductivity detector and an integrator C-R6A (Shimadzu Corp.) with oven temperature of 50 °C. The reaction gas went through a molecular sieve 5 A column (GL Sciences Inc., Japan) with argon as a carrier gas [17].

2.7.2. NH_3 determination by cation chromatography

At each time point, the samples were collected and filtrated by Amicon® Ultra-15 Centrifugal Filters-10 K (Merck Millipore) at 5000*g* for 1 h to remove insoluble components. A 1-mL filtrated sample was injected into a cation exchange chromatography (Dionex, USA) using IonPac™ CG12A (4 × 50 mm) as a guard column and IonPac® CS12A (4 × 250 mm) as an analytical column [23]. The concentration of $\mathbf{NH_4^+}$ was calculated based on a calibration curve of standard NH_4Cl.

2.7.3. ^{1}H NMR analysis of NH_3

To determine that NH_3 was produced from N_2 fixation, the reactions were performed under $^{15}N_2$ atmosphere. The production of $^{15}NH_3$ from the reaction systems was monitored by ^{1}H NMR as reported previously [24] with slight modification. After the reactions, the samples were centrifuged and filtrated to remove cell pellets. For NMR sample preparation, 125 μL of the cell-free sample was mixed with 125 μL of 50 μM maleic acid, 50 μL of 4 M H_2SO_4 and 750 μL of DMSO-d_6. Both $^{14}NH_4Cl$ and $^{15}NH_4Cl$ were used as markers. NMR experiments were carried out on a Bruker Avance III 400 MHz NMR spectrometer (Bruker, Germany).

2.8. Cell membrane permeability of reduced viologen ($V^{\bullet+}$)

To investigate cell membrane permeability of reduced $V^{\bullet+}$, a 100-mL cell suspension including a 5-g cell mass was incubated with 10 mM V^{2+} in $Na_2S_2O_4$ solution at 37 °C and 100 rpm shaking. After incubation, cyanobacterial cell pellets were collected and washed twice with 0.9 % NaCl at 10,000g for 5 min to remove extracellular viologen. The cells containing intracellular V^{2+} were mechanically disrupted by the sonication and freeze-thaw methods for 3 cycles in liquid N_2 for 1 min and a 37 °C-water bath for 5 min. Next, the insoluble cell debris was removed by centrifugation at 10,000g for 5 min. The lysate (2 mL) was reacted with TiO_2 (1 mg) in 100 mM Tris-HCl pH 7 under anaerobic condition and irradiated with a 300-W xenon lamp. The existence of intracellular V^{2+} was estimated by a UV-Vis spectrophotometer [17].

2.9. Photobiocatalytic reaction of TiO_2-cyanobacteria

The combination of photocatalyst and biocatalyst was carried out according to our previous report [17,18] with slight modifications. The reaction solution consisting of 100 mM glycerol pH 7, 250 mg of TiO_2, 10 mM MV^{2+} and 5 g cell mass of cyanobacteria was mixed in a quartz reactor. After the reactor was connected to a closed gas circulation system, the atmosphere of the reaction system was evacuated and replaced with 100 % N_2. Under a 300-W xenon lamp (400 mW/cm^2 light source), the amounts of H_2 and N_2 in gas phase were monitored by gas chromatograph as mentioned in *2.7.1.*, while the production of NH_3 in liquid phase was measured by cation exchange chromatography and NMR technique as mentioned in 2.7.2. and 2.7.3., respectively.

2.10. Cell viability determination by β-galactosidase release assay

A 5-g cell mass of cyanobacterium *A. variabilis* was separately incubated with each component (100 mM glycerol pH 7, 10 mM MV^{2+} or 250 mg TiO_2) and the completed system under illumination. Supernatants were collected after centrifugation at 10,000g for 5 min. The leakage of β-galactosidase (β-gal) indicating cell membrane damage was determined in the reaction solution containing 4 mg/mL of colorless substrate *o*-nitrophenyl-*β*-D-galactoside (ONPG) and the supernatant. The formation of the yellow chromophore *o*-nitrophenol (ONP) was measured at the absorbance A_{420} using a UV-Vis spectrophotometer [25].

3. Results and discussion

3.1. Natural system of NH_3 synthesis

In nature, ATP generated from PSI will transfer electrons to Fe protein and [MoFe]-protein for NH_3 production in the presence of N_2 gas. It is clearly understood that cyanobacteria cultivated in nitrogen-deficient AA medium (Cya^{AA}) can provoke the differentiation of heterocyst as a nitrogenase factory compared to cyanobacteria in BG11 medium (Cya^{BG11}) as shown in Fig. S1 in the Supplementary Material. In Fig. 1a, the intracellular nitrogenase activity of cyanobacteria was preliminarily determined by acetylene reduction assay. After 48 h under 5 % acetylene/95 % N_2 atmosphere, only Cya^{AA} possessed acetylene reduction capacity to ethylene, while Cya^{BG11} had no activity. In addition, it was found that cyanobacteria in culture mediums had low N_2 fixation capacity to produce NH_3, reflecting the fundamental role of the Calvin cycle and photosystem I as natural mechanisms of NH_3 production through ATP-dependent electron transfer from photosynthesis. In comparison, Cya^{AA} shows a higher NH_3 production with a rate of 0.066 μmol/h than Cya^{BG11} with a rate of 0.026 μmol/h (Fig. 1b). Increasing the number of heterocysts in Cya^{AA} is effective for increasing NH_3 production compared to Cya^{BG11} (Fig. S2 in the Supplementary Material). Although the formation of NH_3 was observed, the amount of NH_3 formation was small because of the slow rate of natural N_2 reduction to NH_3 synthesis [7] as described in schematic illustration of Fig. 1c. In this study, inorganic photocatalytic system with viologens as redox mediators was investigated for replacing of Calvin cycle.

3.2. Photocatalytic reduction of viologens by TiO_2

In the light reaction, instead of the Calvin cycle, TiO_2 as an inorganic photocatalyst was able to transfer photoexcited electrons to viologen (V^{2+}) as an electron mediator (Fig. 2). In the principle of viologen photoreduction ($V^{2+} \rightarrow V^{\bullet+}$) induced by photocatalyst, sacrificial reagents, as electron donors/hole scavengers, are required to enhance

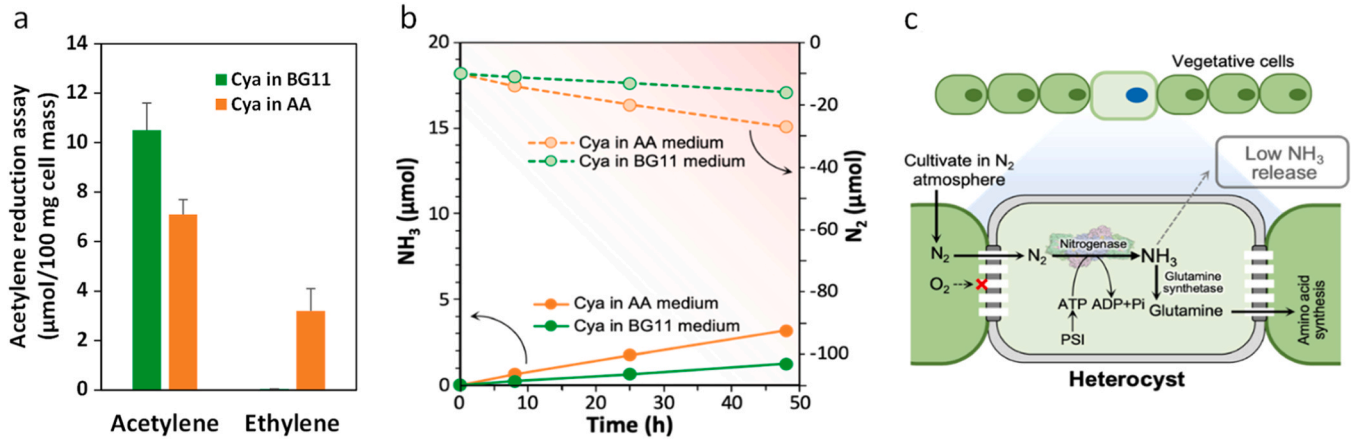

Fig. 1. Bio-natural system of NH_3 production from cyanobacterium *A. variabilis* cultivated in different mediums. (a) Intracellular nitrogenase activity of cyanobacteria in BG11 and AA mediums determined by acetylene reduction assay after 48 h incubating under 5 % acetylene/95 % N_2 atmosphere. (b) Kinetic plots of NH_3 production and N_2 consumption from cyanobacteria (Cya) cultivated in AA medium or BG11 medium at ambient temperature under illumination. (c) Scheme of bio-natural system represents N_2 fixation to NH_3 production in a heterocyst of filamentous cyanobacterial cells.

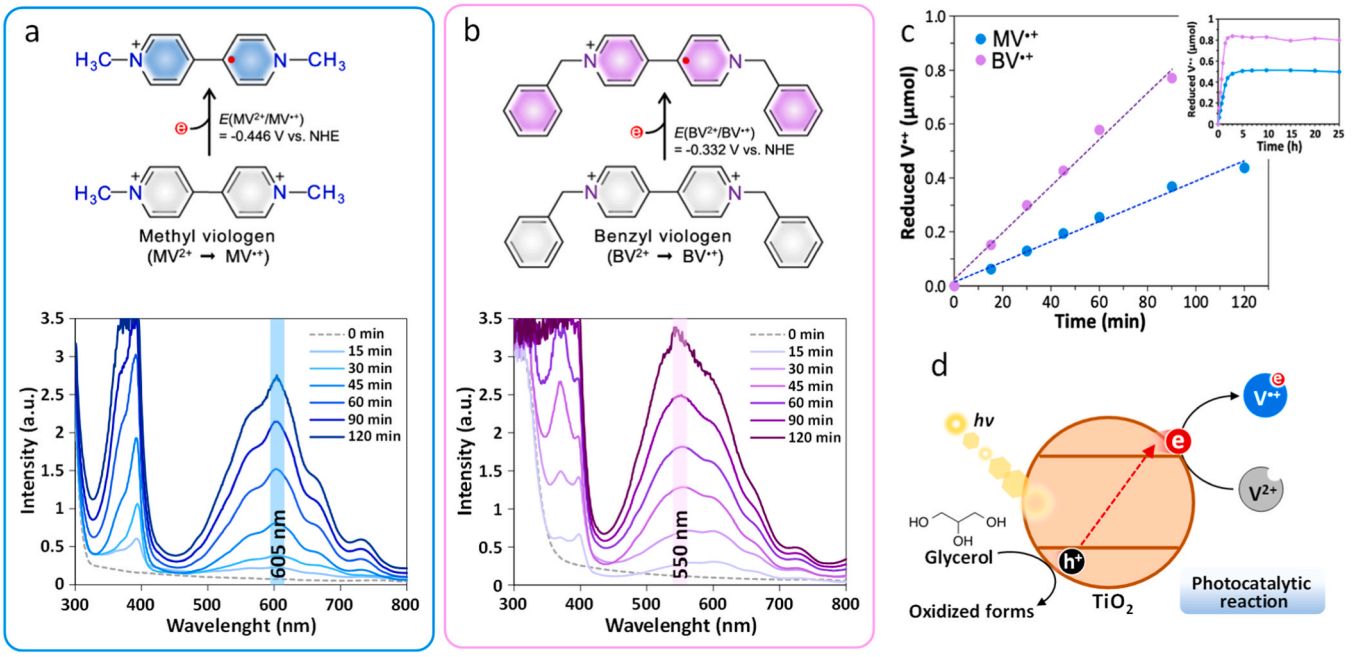

Fig. 2. Photocatalytic reduction of different viologens by TiO_2. The reactions were performed in the mixture including 100 mM glycerol pH 7, 2.5 mg/mL TiO_2 and 10 mM V^{2+} in anaerobic condition under a full arc 300-W xenon illuminator (400 mW/cm^2). (a) Chemical structures of methyl viologen (MV^{2+}→$MV^{\bullet+}$) and UV-Vis spectra of reduced $MV^{\bullet+}$ in a function of time. (b) Chemical structures of benzyl viologen (BV^{2+}→ $BV^{\bullet+}$) and UV-Vis spectra of reduced $BV^{\bullet+}$ in a function of time. (c) The amount of reduced $MV^{\bullet+}$ and $BV^{\bullet+}$ were calculated from UV-Vis spectra at the absorbance of 605 and 550 nm, respectively. Kinetic plots of reduced $V^{\bullet+}$ formation were shown in a time-dependent manner. (d) Scheme of photocatalytic $V^{\bullet+}$ reduction by TiO_2 in the presence of glycerol as a sacrificial reagent under illumination. Data represent the average from three independent measurements with the error bar of standard deviation.

water splitting activity in artificial photosynthesis and prevent the $\mathbf{e}_{CB}^{-}$/$\mathbf{h}_{VB}^{+}$ recombination so-called backward reaction, resulting in the increase of quantum efficiencies [26]. Different biocompatible sacrificial reagents were applied in photoreduction of $V^{\bullet+}$ by TiO_2 as shown in our previous reports [17]. Although Tris, TEOA and Bis-Tris showed greater activity as hole scavengers, glycerol ($C_3H_8O_3$) was selected to avoid the existence of an amine group (-NH_2) that may be decomposed to form NH_3 during the reaction [27]. In addition, it was reported that glycerol was the best hole scavenger with the lowest oxidation potential compared to other alcohols [28].

This study was carried out to determine the photoreduction activities of methyl viologen (MV^{2+}) and benzyl viologen (BV^{2+}) in the reaction mixture including 100 mM glycerol at pH 7, 2.5 mg/mL TiO_2 and 10 mM V^{2+} under full arc illumination. The formations of reduced $V^{\bullet+}$, appearing in the dark blue of $MV^{\bullet+}$ and the purple of $BV^{\bullet+}$, were quantified at characteristic absorption peaks of 605 nm (Fig. 2a) and 550 nm (Fig. 2b) monitored by UV-Vis spectrophotometer, respectively [17]. Linear increase of reduced $BV^{\bullet+}$ formation with the rate of 0.516 ± 0.068 µmol/h was observed at the first 1.5 h after light irradiation, which was about 2.3 times faster than the formation of reduced $MV^{\bullet+}$ with the rate of 0.222 ± 0.041 µmol/h (Fig. 2c).

Theoretically, the valence band edge potential (E_{VB}) of photocatalyst must be more positive than the oxidation potential (E_{ox}) of the sacrificial reagent (D), $E_{VB} > E(D/D^{\bullet+})$ for donating electrons to the valence band holes ($\mathbf{h}_{VB}^{+}$), and the conduction band edge potential (E_{CB}) of photocatalyst must be more negative than the redox potential of viologens as electron mediators ($E_{CB} < E(V^{2+}/V^{\bullet+})$ for accepting photoexcited electron ($\mathbf{e}_{CB}^{-}$) [26,29,30]. According to the above reason, glycerol at pH 7 with E_{ox} of ca. − 0.409 V vs NHE [28] can consume $\mathbf{h}_{VB}^{+}$ in TiO_2 with E_{VB} of ca. 2.447 V vs NHE [31], while TiO_2 with E_{CB} of ca. − 0.653 V vs NHE at pH 7 [31] can transfer the photoexcited $\mathbf{e}_{CB}^{-}$ to both MV^{2+} and BV^{2+} with $E(V^{2+}/V^{\bullet+})$ of − 0.446 and − 0.332 V vs. NHE, respectively [32,33], subsequently $\mathbf{e}_{CB}^{-}/\mathbf{h}_{VB}^{+}$ is charge separated. Therefore, the results reveal that the viologen reduction rate is strongly dependent on the potential separation between TiO_2 E_{CB} and the reduction potential of viologen. Mechanism of photocatalytic $V^{\bullet+}$ reduction by TiO_2 was illustrated in Fig. 2d and presented as follow:

$$\text{Glycerol} + TiO_2 \xrightarrow{h\nu} \underset{(\text{other oxidized } compounds)}{\text{Glyceraldehyde}} + TiO_2 * (\mathbf{h}_{VB}^{+} + \mathbf{e}_{CB}^{-}) \quad (1)$$

$$\mathbf{e}_{CB}^{-} + V^{2+}(\text{oxidized } form) \rightarrow V^{\bullet+} + (\text{reduced } form) \quad (2)$$

3.3. Biocatalytic reaction of cyanobacteria

The first investigation on whole-cell biocatalysts was carried out to ascertain whether culture mediums affect biocatalytic enzyme expression. Both hydrogenase and nitrogenase are metalloenzymes including [NiFe]- and [MoFe]-bimetal active sites, respectively. ICP-AES method was utilized to quantify the existence of biocatalysts based on the contents of specific metal atoms. The results showed that no significant difference was observed in Fe contents (Fig. 3a), while BG11 medium mainly promoted the accumulation of Ni contents (Fig. 3b), indicating the presence of [NiFe]-hydrogenase in cyanobacteria. In contrast, Mo content was significantly increased in cyanobacteria cultivated in AA medium, implying the predominant expression of [MoFe]-nitrogenase (Fig. 3c). Considering the medium ingredients in Table S1 in the Supplementary Material, it can be described that AA medium without N-source stimulates the differentiation of heterocyst for [MoFe]-nitrogenase expression [34]. To verify the activity of nitrogenase and avoid the influence of medium ingredients, cyanobacterial cells were resuspended in 50 mM Tris-HCl pH 7 and incubated under 5 % acetylene/95 % N_2 atmosphere. In Fig. 3d, the results confirmed that only Cya^{AA} with higher Mo content (118.3 ± 17.3 nmol/g cell mass) can produce ethylene from the acetylene reduction with the rate of 0.136 µmol/h, while the activity of Cya^{BG11} with lower Mo content (10.19

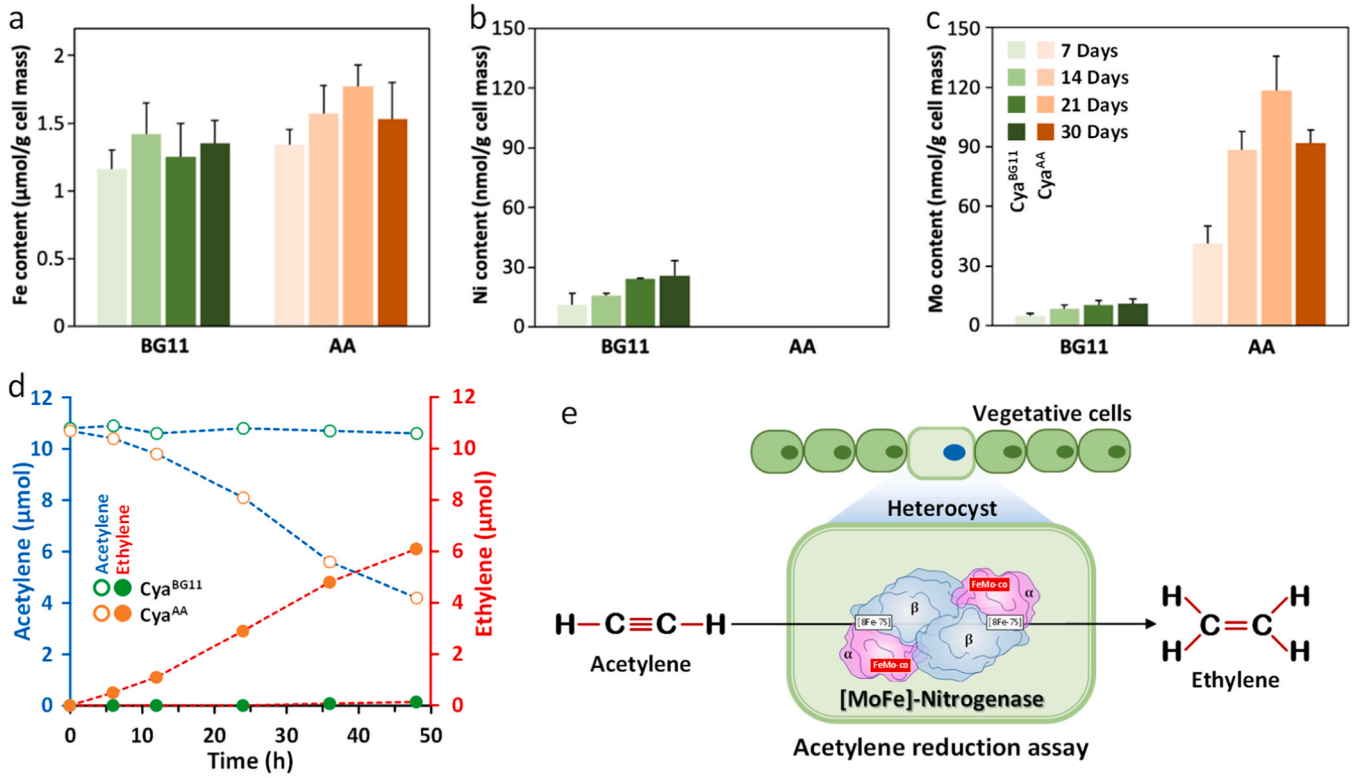

Fig. 3. Intracellular metal ion accumulations of cyanobacterium *A. variabilis* cultivated in BG11 and AA mediums. During cultivation for 7, 14, 21 and 30 Days, a 1-g cell pellet was collected and resuspended in 5 mL of deionized distilled water. Intracellular accumulation of (a) Fe, (b) Ni and (c) Mo contents were quantified by an inductively coupled plasma-atomic emission spectroscopy (ICP-AES) using the calibration curves of Fe, Ni, and Mo standards as shown in Fig. S3 in the Supplementary Material. (d) Nitrogenase activity was determined by acetylene reduction assay. Kinetic plots of acetylene to ethylene conversion was presented in a function of time. (e) Scheme of acetylene reduction to ethylene production by cyanobacterial nitrogenase. Data represent the average from three independent measurements with the error bar of standard deviation.

± 2.43 nmol/g cell mass) was almost zero. Therefore, Cya^{AA} with active [MoFe]-protein was selected for studying the biological-related mechanism of NH_3 production. According to the results, the acetylene reduction activity of cyanobacterial *A. variabilis* was illustrated as shown in Fig. 3e.

Viologens were widely used as soluble electron mediators in many models for carrying the photoexcited e^-_{CB} from photocatalysts to biocatalysts [35,36]. Although both $MV^{\bullet+}$ and $BV^{\bullet+}$ can receive photoexcited electrons from the conduction band of TiO_2 in the photocatalytic reaction, $V^{\bullet+}$-dependent biocatalytic activities of whole-cell system strongly depend on cell permeability and redox potential of viologens as well as cell morphology. Our previous study [17] showed that the bacterial cell envelope is an inherent barrier that restricts the cellular permeability of viologen. Lower viologen accumulations were detected inside cyanobacterial cells with thicker cell envelopes compared to *E. coli* [37]. Therefore, higher concentrations and longer incubation periods of viologens were applied to enhance the biocatalytic activities of cyanobacteria.

Biocatalytic reactions were performed under N_2 atmosphere to preserve the function of O_2-sensitive enzyme. In the whole-cell system, the cell wall is the first checkpoint that must pass before encountering intracellular biocatalysts. A comparative study showed that the intracellular accumulation of $MV^{\bullet+}$ was about 4.2 times higher than that of $BV^{\bullet+}$ at 25 h, while no viologen accumulation was found in the negative control experiments (Fig. 4a). During the reactions, NH_3/H_2 productions and N_2 consumption were simultaneously measured. As time increases, H_2 was produced from $MV^{\bullet+}$-treated cyanobacterial cells with the rate of 0.70 ± 0.14 μmol/h, while no H_2 generation was observed in $BV^{\bullet+}$-treated cells (Fig. 4b). Although it was reported that both $V^{\bullet+}$ were highly permeant cations with greater lipophilicity over their oxidized forms (V^{2+}) [38], it is evident by this study that only $MV^{\bullet+}$ as a smaller positively-charge molecular can penetrate through the cell envelope. In general, both bidirectional [NiFe]-hydrogenase and [MoFe]-nitrogenase were key intracellular biocatalysts of cyanobacterial H_2 generation. However, no nickel was detected in Cya^{AA} as shown in Fig. 3b, suggesting that [MoFe]-nitrogenase was the only enzyme responsible for H_2 production in this experiment. Based on the results obtained in this case, it is not reasonable to consider only cell permeability of viologens. Difference in redox potentials was considered as one of the main factors. A more negative redox potential of methyl viologen [$E(MV^{2+}/MV^{\bullet+})$ = −0.446 V vs. NHE] [32,33] provided a favorable potential scale for proton reduction with the $E(H^+/H_2)$ of − 0.41 V vs. NHE at pH 7 [39], while the redox potential of benzyl viologen with the $E(BV^{2+}/BV^{\bullet+})$ of − 0.332 V vs. NHE was insufficient for water splitting to H_2 production.

Since NH_3 production is the main purpose of this work, biocatalytic activity of nitrogenase-expressing organisms is important for an initial assessment. In Fig. 4c, the plots between NH_3 production against N_2 consumption showed that only $MV^{\bullet+}$-treated cyanobacterium fixed N_2 for producing NH_3 in a time-dependent manner with the rate of 1.30 ± 0.27 μmol/h, while $BV^{\bullet+}$-treated cyanobacterium has no activities. The results obtained from the $MV^{\bullet+}$-dependent biocatalytic reaction showed the NH_3:H_2 ratio at 1.86 (Fig. 4d). In many circumstances, $MV^{\bullet+}$ has been widely utilized as an in vitro reductant and electrochemical mediator for low-potential oxidoreductases such as hydrogenase [17,18], formate dehydrogenase [40,41] and CO dehydrogenase [42,43] as well as nitrogenase [44]. Based on the results obtained from this study in conjunction with a well-known natural mechanism, $MV^{\bullet+}$-dependent NH_3 production can be demonstrated in the following equation:

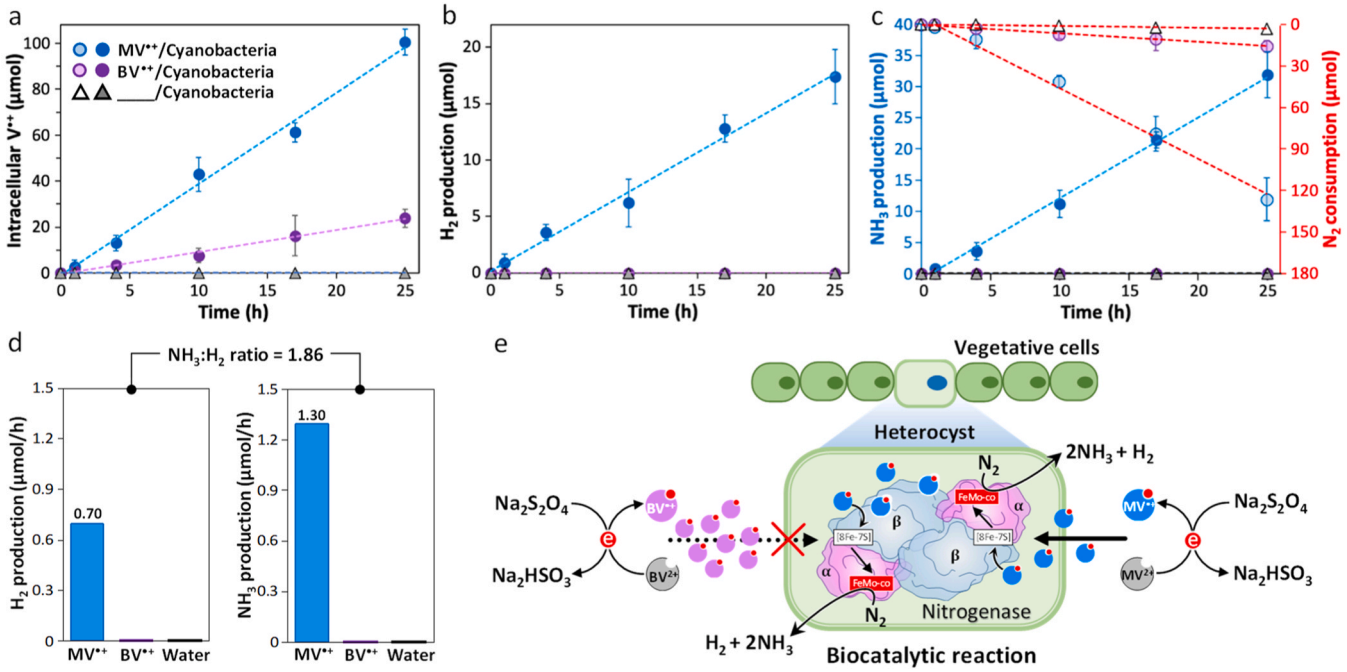

Fig. 4. Biocatalytic reaction of cyanobacterium *A. variabilis*. (a) Time-courses of intracellular $V^{\bullet+}$ accumulations, (b) $V^{\bullet+}$-dependent H_2 production and (c) NH_3 production versus N_2 consumption from the system including 10 mM MV^{2+} in $Na_2S_2O_4$ solution, a 5 g cell mass of cyanobacteria in total volume 100 mL under N_2 atmosphere monitored by cation chromatography and gas chromatograph, respectively. The amount of NH_3 was calculated using the standard plot of NH_4Cl determination as shown in Fig. S4 in the Supplementary Material. (d) Evaluation on NH_3:H_2 ratio of biocatalytic reactions. (e) Scheme of the biocatalytic reaction using different $V^{\bullet+}$ as electron mediators. Data represent the average from three independent measurements with the error bar of standard deviation.

$$N_2 + 8MV^{\bullet+} + 8H^+ \xrightarrow{\text{[MoFe]-Nitrogenase}} 2NH_3 + H_2 + 8MV^{2+} \quad (3)$$

The achievement of two NH_3 molecules per cycle via the function of nitrogenase requires $8e^-$ from 8 $MV^{\bullet+}$ molecules and the reduction of one molecular N_2 as predicted in Fig. 4e. According to the ratio between substrates and products, the following mathematical formula was devised to estimate the efficiency of the system:

$$\text{Efficiency of the system } (\%) = \frac{\text{Number of consumed electrons}}{\text{Number of total electrons used in the system}} \times 100$$

The number of consumed electrons was calculated from the amounts of produced NH_3 and H_2 during experiments:

$$\text{Number of consumed electrons} = (\text{Amount of } NH_3\ (\mu\text{mol}) \times 3) + (\text{Amount of } H_2\ (\mu\text{mol}) \times 2)$$

where '3' was the number of required electrons for one NH3 formation, and '2' was the number of required electrons for one H_2 formation. While the number of total electrons used in the system was equal to the total amount of reduced $MV^{\bullet+}$ (μmol) utilized in the system:

$$\text{Number of total electrons} = \text{Total amount of reduced } MV^{\bullet+}\ (\mu\text{mol})$$

To estimate the efficiency of our whole-cell system, 10 mM of MV^{2+} in a 100 mL of total reaction volume can provide a maximum $MV^{\bullet+}$ content of 1000 μmol (one $MV^{\bullet+}$ molecule carrying a single electron) to produce 250 μmol of NH_3 (require $3e^-$ per molecule) and 125 μmol of H_2 (require $2e^-$ per molecule). However, in practice, 31.9 μmol of NH_3 and 17.4 μmol of H_2 were formed over 25 h, indicating that the system spent 13.1 % of total electrons in form of reduced $MV^{\bullet+}$. It is speculated that the use of natural microorganisms with low productivity of biocatalysts and the thickness of cyanobacterial cell wall might be the two main factors impeding the interaction between electron-carrying reduced $MV^{\bullet+}$ and intracellular nitrogenase. Although NH_3 could be generated from the conditions used in this work, our studies suggest that the whole-cell system should be improved to enhance the biocatalytic enzyme expression and find more suitable hosts through genetic engineering strategies in the future development.

3.4. Photobiocatalytic reaction of TiO_2-cyanobacteria

To achieve the goal of producing NH_3 using light energy, the combination of TiO_2 as a light-absorbed photocatalyst and nitrogenase-expressing cyanobacterium *A. variabilis* was carried out to construct a sustainable system of photobiocatalytic NH_3 production under ambient conditions.

During the reaction of photobiocatalytic NH_3 production, H_2 production and N_2 consumption were simultaneously determined as shown in Fig. 5, Fig. S5 and Table S2 in the Supplementary Material. Among various conditions, results clearly showed that the complete systems significantly enhanced H_2 production. In particular, the system using cyanobacteria grown in BG11 medium (Cya^{BG11}) generated the highest H_2 formation rate of 5.99 ± 0.45 μmol/h (Table S2 in the Supplementary Material). Considering the larger amount of Ni content, hydrogenase in cyanobacteria became larger in BG11 medium and so a higher H_2 formation rate can be assigned to a larger amount of [NiFe]-hydrogenase as shown in Fig. 3b. Lower yields of H_2 were observed in the systems using cyanobacteria cultivated in AA medium (Cya^{AA}) and the systems lacking one of each component (Fig. S5a and Table S2 in the Supplementary Material), i.e., glycerol, MV^{2+} and TiO_2. The complete system of whole-cell Cya^{AA} produced H_2 at the rate of 3.71 ± 0.39 μmol/h (Fig. 5a), while the lack of components showed lower H_2 production rate. In addition, it was found that the addition of MSX (L-methionine sulfoximine), as a glutamine synthetase inhibitor [45–47], showed similar results to the MSX-free complete system suggesting MSX did not affect the activity of nitrogenase or hydrogenase (Table S2 in the Supplementary Material).

To verify that the production of NH_3 was obtained from N_2 fixation, the remaining amount of N_2 in a headspace of the reactor was measured at each time. In Fig. 5b, the significant decrease of N_2 was observed in

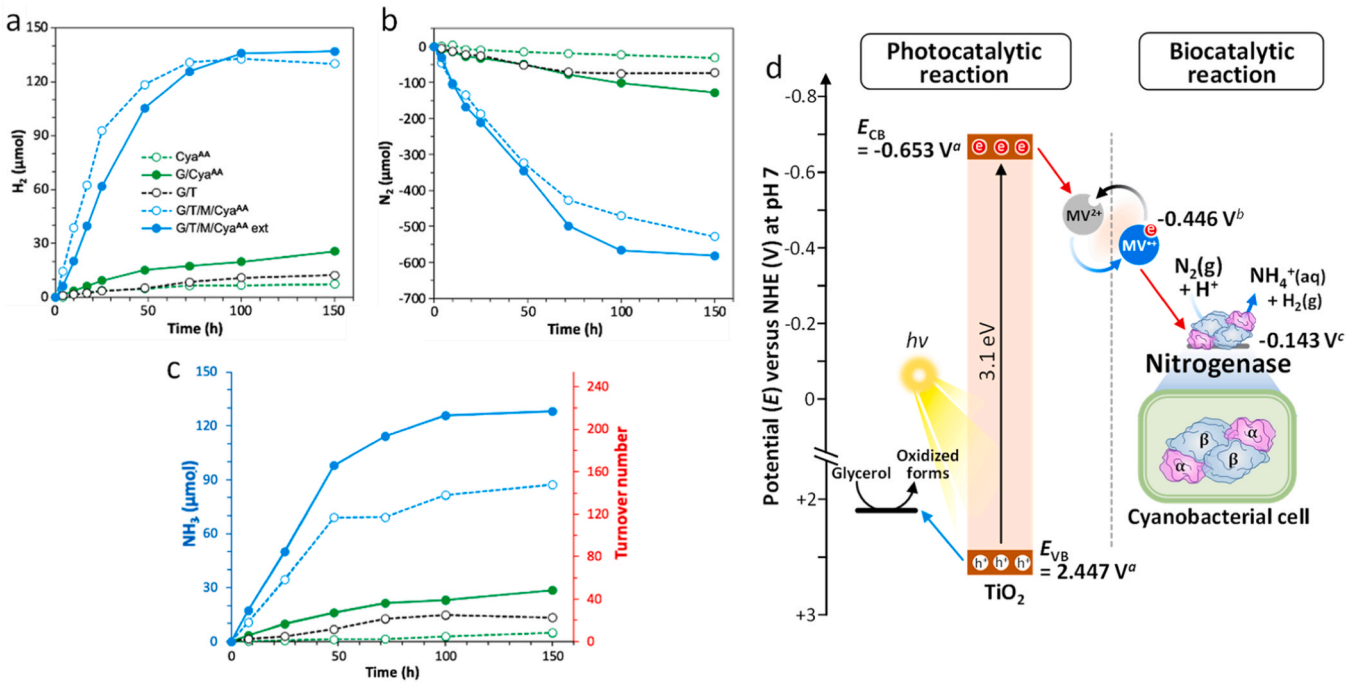

Fig. 5. Photobiocatalytic NH_3 production of cyanobacterium *A. variabilis* coupled to TiO_2 in various conditions. (a) H_2 production, (b) N_2 consumption and (c) the amount and turnover number of NH_3 production were quantified based on the reaction solution consisting of 100 mM glycerol pH 7, 250 mg of TiO_2, 10 mM MV^{2+} and a 5 g cell mass of cyanobacterial cells mixed in a quartz reactor under xenon lamb (400 mM/cm^2). Cya^{AA}, cyanobacterium cultivated in AA medium; G, glycerol; T, TiO_2 and M, methyl viologen (MV^{2+}). Turnover number (TON) indicates the amount of NH_3 per Mo content at each time. Data represent the average from three independent measurements. (d) Scheme of electron transfer processes in photobiocatalytic reaction of NH_3 production. The potentials (*E*) were cited based on the previous published literatures: [a] Ref. [28], [b] Ref. [32] and.

the complete systems of whole-cell Cya^{AA} and its extract with the consumption rate of − 6.49 and − 7.17 μmol/h, respectively. However, very low N_2 consumption was observed in the system of the Cya^{BG11} (−0.70 μmol/h) (Fig. S5b and Table S2 in the Supplementary Material). The decrease in N_2 is one of the primary evidence affirming that N_2 fixation occurred during NH_3 synthesis. Based on the above results, the samples were simultaneously determined to quantify the amount of NH_3 by cation chromatography as shown in Fig. 5c. At 48 h reaction, the complete system of Cya^{AA} extract showed the maximum NH_3 production rate of 2031.7 nmol/h (33.86 nmol/min) that significantly increased 81.3 times compared to the natural efficiency of Cya^{AA} alone.

Considering on Mo contents, Cya^{AA} with much larger amount of [MoFe]-protein (118.3 ± 17.3 nmol Mo/g cell mass) produced a larger amount of NH_3 from the hybrid system coupled to TiO_2 with the maximum turnover number (TON) of 216.8 at 150 h. However, the formation rate of NH_3 in the system of Cya^{BG11} (containing only 10.19 ± 2.43 nmol Mo/g cell mass) was just 150 nmol/h. Thus, the photobiocatalysis of TiO_2-Cya^{AA} system significantly increased the formation of NH_3. Because the intracellular NH_3 is a main N-source of amino acid synthesis [48], the addition of an inhibitor of glutamine synthetase, MSX, was further effective for NH_3 accumulation with the rate of 1650 nmol/h compared to the complete system of whole cells without MSX (Figs. S5c, S6 and Table S2 in the Supplementary Material).

For the role of glycerol, change in glycerol was further analysed with NMR in D_2O at pH= 7 before and after reaction. As shown in Fig. S7 in the Supplementary Material, only glycerol was detected before the reaction started, while NMR peaks of glyceraldehyde and dihydroxyacetone appeared after reaction, corresponding to the previous report [49]. So, it confirms that glycerol works as sacrificial reagent which is a hole scavenger to TiO_2. It is also noted that amount of NH_3 formation became much smaller when no MV^{2+} was added in the system as shown in Table S2 in the Supplementary Material. So, NH_3 is mainly formed on biocatalyst, but not on TiO_2 with glycerol.

As shown in Fig. 5, the production of H_2 and NH_3 gradually becomes saturated because the amount of glycerol as a hole scavenger decreases to be insufficient with time. In addition, deactivation of nitrogenase might be another reason. Although the photocatalytic reaction was performed at neutral pH (pH 7), prolong exposure to harsh environments can cause damage to cellular structures and biomolecules. It was verified by *β*-galactosidase release cytotoxic assay as shown in Fig. S8 in the Supplementary Material that 32.6 % of cell damage was observed after 48-h reaction. Therefore, nitrogenase, as a biocatalytic enzyme, may be gradually deactivated in highly-concentrated organic solution with pH change (pH 5–6 after reaction) and also the accumulation of oxidative products from glycerol oxidation because nitrogenase is

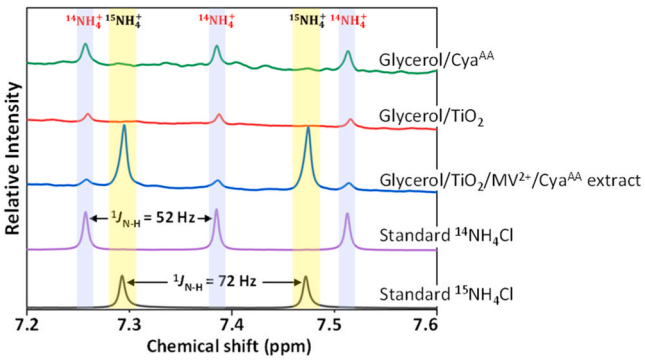

Fig. 6. ^1H NMR analysis of $^{14}NH_3$ and $^{15}NH_3$. Photobiocatalytic system consists of 100 mM glycerol pH 7, 250 mg of TiO_2, 10 mM MV^{2+} and Cya^{AA} extract from a 5 g cell mass mixed in a quartz reactor under illumination (400 mM/cm^2) and $^{15}N_2$ atmosphere. ^1H NMR analysis was performed to verify the formation of $^{15}NH_3$ from $^{15}N_2$ gas fixation compared to the standard solutions of $^{14}NH_4Cl$ and $^{15}NH_4Cl$.

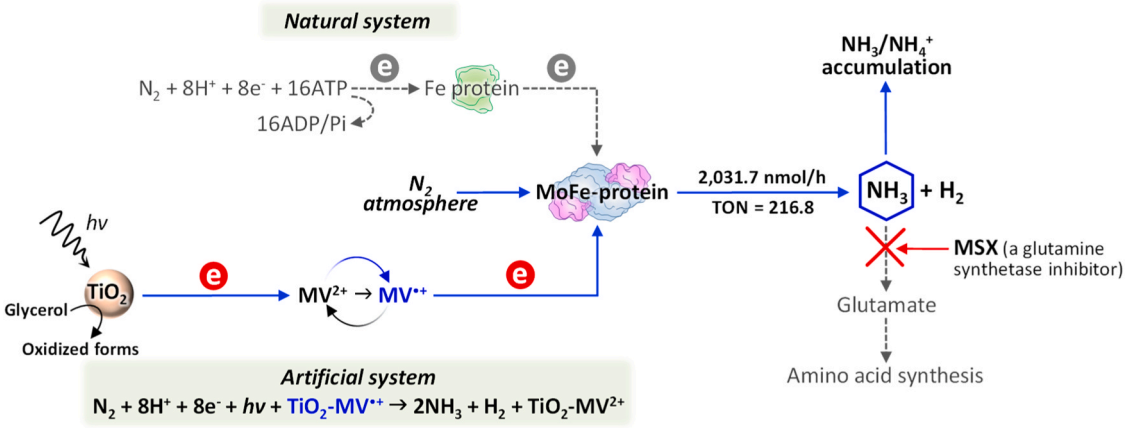

Fig. 7. NH_3 production of natural and artificial photobiocatalytic systems. Cyanobacterial [MoFe]-nitrogenase is a key biocatalytic enzyme for N_2 reduction to NH_3 synthesis. The natural system requires ATP and Fe protein for electron transfer process to [MoFe]-protein. The artificial photobiocatalysis of TiO_2 coupled to [MoFe]-nitrogenase is an ATP-free mechanism performed in the presence of glycerol as a sacrificial reagent and methyl viologen ($MV^{2+} \rightarrow MV^{\bullet+}$) as an electron mediator under light source and ambient conditions.

unstable in oxidation environment. All experimental results support the reaction mechanism of the photobiocatalytic NH_3 production as schematically shown in Fig. 5d, corresponding to the redox potentials of each constituent as report previously [28,32,50].

[c] Ref. 50, where the values at pH 7 were estimated from the Nernst equation: $E = E_0 - 0.059$ pH.

In order to confirm gaseous N_2 fixation to NH_3 synthesis, the reaction was performed under $^{15}N_2$ atmosphere and detected by ^1H NMR method. Since the chemical shift and number of peaks were different between NMR spectra of $^{14}NH_3$ and $^{15}NH_3$, we can characterize and identify the presence of $^{15}NH_3$ in the samples [24]. In Fig. 6, only $^{14}NH_3$ was detected in the samples of Cya^{AA} or TiO_2 in glycerol solution, while the formation of $^{15}NH_3$ was obviously detected in the complete system of glycerol/TiO_2/MV^{2+}/Cya^{AA} extract. According to the results, it confirms that NH_3 was synthesized from gaseous N_2 as a N-source and H_2O via the activity of cyanobacterial nitrogenase.

NH_3 decomposition was measured in the reaction under Ar atmosphere, which is the backward reaction. By addition external NH_3 solution to the complete photobiocatalytic system, no significant changes in NH_3 content and no N_2 generation were observed during the 48-h reaction as shown in Fig. S9 in the Supplementary Material. Therefore, it confirms that the decomposition of NH_3 by the hole of TiO_2 seems to be occurred negligibly. This could be assigned to removal of hole in TiO_2 effectively by glycerol.

For better understanding, the success of the artificial photobiocatalytic system with ATP-free reaction developed in this study was compared with ATP-dependent natural mechanism [51] as shown in Fig. 7 and Fig. S6 in the Supplementary Material. In this newly proposed system, by replacing the slow process of natural Calvin cycle in cyanobacterial cells with the faster reduction rate of TiO_2 photocatalyst, a higher rate of NH_3 synthesis was reasonably achieved at 2031.7 nmol/h with TON of 216.8. The rate and total amount of NH_3 production in our system are much larger than those reported by other group as shown in Table S3.

4. Conclusion

Due to the environmental crisis and high energy consumption caused by the current NH_3 production industry, it is a challenge for scientists to develop alternative technologies that are environmentally friendly. Photobiocatalytic system is one of the attempts to use light energy for NH_3 synthesis through the action of cyanobacterial nitrogenase. In the photocatalytic reaction, glycerol as a sacrificial electron donor and a hole scavenger of TiO_2 is necessary for accelerating the reductions of electron mediators: $MV^{\bullet+}$ and $BV^{\bullet+}$. However, studies on the biocatalytic reaction revealed that only $MV^{\bullet+}$ was able to penetrate the cell envelope and transfer electrons for H_2 and NH_3 productions by [MoFe]-nitrogenase-rich cyanobacteria cultivated in AA medium (Cya^{AA}). Various conditions of the hybrid system studies confirmed the crucial roles of each component in increasing N_2 fixation to NH_3 production. The best condition was achieved at the maximum NH_3 production rate of 2031.7 nmol/h with TON of 216.8 in the presence of glycerol, TiO_2, MV^{2+}, and cyanobacterial cell extract under light energy at ambient conditions. This study provides evidence that the cyanobacterium *A. variabilis* is suitable to be further developed for photobiocatalytic NH_3 production. The achievement of the TiO_2-cyanobacterium hybrid system guides us toward the construction of a sustainable NH_3 production with extremely cheap and green processes.

CRediT authorship contribution statement

Nuttavut Kosem: Conceptualization, Investigation, Methodology, Writing – original draft. **Xiao-feng Shen:** NMR analysis and Software. **Yutaka Ohsaki:** Bacterial cultivation, Nitrogenase activity assay. **Motonori Watanabe:** NMR software and Validation, Writing – review & editing. **Jun Tae Song:** Methodology. **Tatsumi Ishihara:** Supervision, Funding acquisition, Resources, Writing – review & editing.

Declaration of Competing Interest

The authors declare that they have no known competing financial interests or personal relationships that could have appeared to influence the work reported in this paper.

Data availability

No data was used for the research described in the article.

Acknowledgements

This study was financially supported by a Grant-in-Aid for Grant-in-Aid for Challenging Exploratory Research from the Ministry of Education, Culture, Sports, Science and Technology (MEXT), Japan through the Japan Society for the Promotion of Science (21K18213).

Appendix A. Supporting information

Supplementary data associated with this article can be found in the online version at doi:10.1016/j.apcatb.2023.123431.

References

[1] R.D. Milton, R. Cai, S. Abdellaoui, D. Leech, A.L. De Lacey, M. Pita, S.D. Minteer, Bioelectrochemical Haber-Bosch process: an ammonia-producing H_2/N_2 fuel cell, Angew. Chem. Int. Ed. 56 (2017) 2680–2683.

[2] V. Kyriakou, I. Garagounis, A. Vourros, E. Vasileiou, M. Stoukides, An electrochemical Haber-Bosch process, Joule 4 (2020) 142–158.

[3] W. Gu, R.D. Milton, Natural and engineered electron transfer of nitrogenase, Chemistry 2 (2020) 322–346.

[4] J.F. Ortiz-Medina, A.M. Grunden, M.R. Hyman, D.F. Call, Nitrogen gas fixation and conversion to ammonium using microbial electrolysis cells, ACS Sustain. Chem. Eng. 7 (2019) 3511–3519.

[5] S. Zhang, Y. Zhao, R. Shi, G.I.N. Waterhouse, T. Zhang, Photocatalytic ammonia synthesis: recent progress and future, EnergyChem 1 (2019), 100013.

[6] C.J.M. van der Ham, M.T.M. Koper, D.G.H. Hetterscheid, Challenges in reduction of dinitrogen by proton and electron transfer, Chem. Soc. Rev. 43 (2014) 5183–5191.

[7] M.I. Muro-Pastor, F.J. Florencio, Regulation of ammonium assimilation in cyanobacteria, Plant Physiol. Biochem. 41 (2003) 595–603.

[8] K.A. Brown, D.F. Harris, M.B. Wilker, A. Rasmussen, N. Khadka, H. Hamby, S. Keable, G. Dukovic, J.W. Peters, L.C. Seefeldt, P.W. King, Light-driven dinitrogen reduction catalyzed by a CdS:nitrogenase MoFe protein biohybrid, Science 352 (2016) 448–450.

[9] L. Wang, M. Xia, H. Wang, K. Huang, C. Qian, C.T. Maravelias, G.A. Ozin, Greening ammonia toward the solar ammonia refinery, Joule 2 (2018) 1055–1074.

[10] K.A. Brown, J. Ruzicka, H. Kallas, B. Chica, D.W. Mulder, J.W. Peters, L.C. Seefeldt, G. Dukovic, P.W. King, Excitation-rate determines product stoichiometry in photochemical ammonia production by CdS quantum dot-nitrogenase MoFe protein complexes, ACS Catal. 10 (2020) 11147–11152.

[11] S. Koh, Y. Choi, I. Lee, G.-M. Kim, J. Kim, Y.-S. Park, S.Y. Lee, D.C. Lee, Light-driven ammonia production by *Azotobacter vinelandii* cultured in medium containing colloidal quantum dots, J. Am. Chem. Soc. 144 (2022) 10798–10808.

[12] J. Elhai, C.P. Wolk, Developmental regulation and spatial pattern of expression of the structural genes for nitrogenase in the cyanobacterium *Anabaena*, EMBO J. 9 (1990) 3379–3388.

[13] T. Thiel, Organization and regulation of cyanobacterial *nif* gene clusters: implications for nitrogenase expression in plant cells, FEMS Microbiol. Lett. 366 (2019), fnz077.

[14] T. Watanabe, T. Horiike, The evolution of molybdenum dependent nitrogenase in cyanobacteria, Biology 10 (2021) 329.

[15] C.W. Mullineaux, V. Mariscal, A. Nenninger, H. Khanum, A. Herrero, E. Flores, D. G. Adams, Mechanism of intercellular molecular exchange in heterocyst-forming cyanobacteria, EMBO J. 27 (2008) 1299–1308.

[16] A.M. Muro-Pastor, W.R. Hess, Heterocyst differentiation: from single mutants to global approaches, Trends Microbiol. 20 (2012) 548–555.

[17] N. Kosem, M. Watanabe, J.T. Song, A. Takagaki, T. Ishihara, A comprehensive study on rational biocatalysts and individual components of photobiocatalytic H_2 production systems, Appl. Catal. A Gen. 651 (2023), 119019.

[18] Y. Honda, M. Watanabe, H. Hagiwara, S. Ida, T. Ishihara, Inorganic/whole-cell biohybrid photocatalyst for highly efficient hydrogen production from water, Appl. Catal. B Environ. 210 (2017) 400–406.

[19] J. Heider, K. Ma, M.W.W. Adams, Purification, characterization, and metabolic function of tungsten-containing aldehyde ferredoxin oxidoreductase from the hyperthermophilic and proteolytic archaeon *Thermococcus* strain ES-1, J. Bacteriol. 17 (1995) 4757–4764.

[20] H. Masukawa, H. Sakurai, R.P. Hausinger, K. Inoue, Increased heterocyst frequency by patN disruption in *Anabaena* leads to enhanced photobiological hydrogen production at high light intensity and high cell density, Appl. Microbiol. Biotechnol. 101 (2017) 2177–2188.

[21] K. Gutekunst, D. Hoffmann, U. Westernströer, R. Schulz, D. Garbe-Schönberg, J. Appel, In-vivo turnover frequency of the cyanobacterial NiFe-hydrogenase during photohydrogen production outperforms in-vitro systems, Sci. Rep. 8 (2018) 6083.

[22] M. Staal, S. te Lintel-Hekkert, F. Harren, L. Stal, Nitrogenase activity in cyanobacteria measured by the acetylene reduction assay: a comparison between batch incubation and on-line monitoring, Environ. Microbiol. 3 (2001) 343–351.

[23] H. Hirakawa, M. Hashimoto, Y. Shiraishi, T. Hirai, Photocatalytic conversion of nitrogen to ammonia with water on surface oxygen vacancies of titanium dioxide, J. Am. Chem. Soc. 139 (2017) 10929–10936.

[24] R.Y. Hodgetts, A.S. Kiryutin, P. Nichols, H.-L. Du, J.M. Bakker, D.R. Macfarlane, A. N. Simonov, Refining universal procedures for ammonium quantification via rapid ^{1}H NMR analysis for dinitrogen reduction studies, ACS Energy Lett. 5 (2020) 736–741.

[25] K.L. Griffith, R.E. Wolf Jr., Measuring β-galactosidase activity in bacteria: cell growth, permeabilization, and enzyme assays in 96-well arrays, Biochem. Biophys. Res. Commun. 290 (2002) 397–402.

[26] M. Ni, M.K.H. Leung, D.Y.C. Leung, K. Sumathy, A review and recent developments in photocatalytic water-splitting using TiO_2 for hydrogen production, Renew. Sustain. Energy Rev. 11 (2007) 401–425.

[27] A. Bandyopadhyay, J. Stöckel, H. Min, L.A. Sherman, H.B. Pakrasi, High rates of photobiological H_2 production by a cyanobacterium under aerobic conditions, Nat. Commun. 1 (2010) 139.

[28] Z.H.N. Al-Azri, W.-T. Chen, A. Chan, V. Jovic, T. Ina, H. Idriss, G.I.N. Waterhouse, The roles of metal co-catalysts and reaction media in photocatalytic hydrogen production: performance evaluation of M/TiO_2 photocatalysts (M = Pd, Pt, Au) in different alcohol–water mixtures, J. Catal. 329 (2015) 355–367.

[29] O.L. Stroyuk, O.Ye Rayevska, A.V. Kozytskiy, S.Ya Kuchmiy, Electron energy factors in photocatalytic methyl viologen reduction in the presence of semiconductor nanocrystals, J. Photochem. Photobiol. A. 210 (2010) 209–214.

[30] M. Wang, S. Shen, L. Li, Z. Tang, J. Yang, Effects of sacrificial reagents on photocatalytic hydrogen evolution over different photocatalysts, J. Mater. Sci. 52 (2017) 5155–5164.

[31] S. Taghavi, A. Amoozadeh, F.J. Nemati, The first report of deep eutectic solvent (DES) nano-photocatalyst (n-TiO_2-P25@TDI@DES (urea: $ZnCl_2$)) and its application on selective oxidation of benzyl alcohols to benzaldehydes, J. Chem. Technol. Biotechnol. 96 (2020) 384–393.

[32] D.L. Erbes, R.H. Burris, The kinetics of methyl viologen oxidation and reduction by the hydrogenase from *Clostridium pasteurianium*, Biochim. Biophys. Acta 525 (1978) 45–54.

[33] S.M. Kim, J.H. Jang, K.K. Kim, H.K. Park, J.J. Bae, W.J. Yu, I.H. Lee, G. Kim, D. D. Loc, U.J. Kim, E.-H. Lee, H.-J. Shin, J.-Y. Choi, Y.H. Lee, Reduction-controlled viologen in bisolvent as an environmentally stable n-type dopant for carbon nanotubes, J. Am. Chem. Soc. 131 (2009) 327–331.

[34] H. Berberoğlu, J. Jay, L. Pilon, Effect of nutrient media on photobiological hydrogen production by *Anabaena variabilis* ATCC 29413, Int. J. Hydrog. Energy 33 (2008) 1172–1184.

[35] S.H. Lee, J.H. Kim, C.B. Park, Coupling photocatalysis and redox biocatalysis toward biocatalyzed artificial photosynthesis, Chem. Eur. J. 19 (2013) 4392–4406.

[36] S. Shi, C. Zeng, T. Si, B. Wang, P.K. Wong, Photobiocatalytic solar fuel and solar chemical conversion: sufficient activity and better selectivity, ACS EST Eng. 2 (2022) 989–1000.

[37] K.K. Mehta, N.H. Evitt, J.R. Swartz, Chemical lysis of cyanobacteria, J. Biol. Eng. 9 (2015) 10.

[38] R.W. Jones, T.A. Gray, P.B. Garland, A study of the permeability of the cytoplasmic membrane of *Escherichia coli* to reduced and oxidized benzyl viologen and methyl viologen cations: complications in the use of viologens as redox mediators for membrane-bound enzymes, Biochem. Soc. Trans. 4 (1976) 671–673.

[39] Z.J. Jay, K.A. Hunt, K.J. Chou, G.J. Schut, P.-C. Maness, M.W.W. Adams, R. P. Carlson, Integrated thermodynamic analysis of electron bifurcating [FeFe]-hydrogenase to inform anaerobic metabolism and H_2 production, Biochim. Biophys. Acta Bioenerg. 1861 (2020), 148087.

[40] S. Kuwabata, R. Tsuda, H. Yoneyama, Electrochemical conversion of carbon dioxide to methanol with the assistance of formate dehydrogenase and methanol dehydrogenase as biocatalysts, J. Am. Chem. Soc. 116 (1994) 5437–5443.

[41] H.G. Enoch, R.L. Lester, The purification and properties of formate dehydrogenase and nitrate reductase from *Escherichia coli*, J. Biol. Chem. 250 (1975) 6693–6705.

[42] W. Shin, S.H. Lee, J.W. Shin, S.P. Lee, Y. Kim, Highly selective electrocatalytic conversion of CO_2 to CO at –0.57 V (NHE) by carbon monoxide dehydrogenase from *Moorella thermoacetica*, J. Am. Chem. Soc. 125 (2003) 14688–14689.

[43] J. Hadj-Saïd, M.-E. Pandelia, C. Léger, V. Fourmond, S. Dementin, The carbon monoxide dehydrogenase from *Desulfovibrio vulgaris*, Biochim. Biophys. Acta Bioenerg. 1847 (2015) 1574–1583.

[44] A. Badalyan, Z.-Y. Yang, B. Hu, J. Luo, M. Hu, T.L. Liu, L.C. Seefeldt, An efficient viologen-based electron donor to nitrogenase, Biochemistry 58 (2019) 4590–4595.

[45] J.W. Newton, J.F. Cavins, Liberation of ammonia during nitrogen fixation by a facultatively heterotrophic cyanobacterium, Biochim. Biophys. Acta Bioenerg. 809 (1985) 44–50.

[46] S. Boussiba, J. Gibson, Ammonia translocationin cyanobactcria, FEMS Microbiol. Rev. 88 (1991) 1–14.

[47] A.K. Singh, M.B. Syiem, R.S. Singh, S. Adhikari, A.N. Rai, A common transport system for methionine, L-methionine-DL-sulfoximine (MSX), and phosphinothricin (PPT) in the diazotrophic cyanobacterium *Nostoc muscorum*, Curr. Microbiol. 56 (2008) 436–441.

[48] A.A. Esteves-Ferreira, M. Inaba, A. Forta, W.L. Araújo, R. Sulpicea, Nitrogen metabolism in cyanobacteria: metabolic and molecular control, growth consequences and biotechnological applications, Crit. Rev. Microbiol. 44 (2018) 541–560.

[49] T. Jedsukontorn, V. Meeyoo, N. Saito, M. Hunsom, Route of glycerol conversion and product generation via TiO_2-induced photocatalytic oxidation in the presence of H_2O_2, Chem. Eng. J. 281 (2015) 252–264.

[50] Y. Huang, N. Zhang, Z. Wu, X. Xie, Artificial nitrogen fixation over bismuth-based photocatalysts: fundamentals and future perspectives, J. Mater. Chem. A 8 (2020) 4978–4995.

[51] T.D. Rapson, C.C. Wood, Analysis of the ammonia production rates by nitrogenase, Catalysts 12 (2022) 844.